

Magnetic Exchange in Dinuclear Chromium(II) Complexes: Effect of Bridging Chlorides and Bridging Hydrides in Antiferromagnetic Coupling

Michael D. Fryzuk,* Daniel B. Leznoff,† Steven J. Rettig,‡ and Robert C. Thompson*

Department of Chemistry, University of British Columbia, 2036 Main Mall, Vancouver, BC, Canada V6T 1Z1

Received May 26, 1994[⊗]

The preparation, solid-state structures, and magnetic properties of two new Cr(II) amido diphosphine complexes are described. Reaction of the lithium salt $\text{LiN}(\text{SiMe}_2\text{CH}_2\text{PPh}_2)_2$ with $\text{CrCl}_2\cdot\text{THF}$ results in the formation of the dinuclear chloride-bridged species $\{[(\text{Ph}_2\text{PCH}_2\text{SiMe}_2)_2\text{N}]\text{Cr}\}_2(\mu\text{-Cl})_2$, **1**. This complex is paramagnetic at room temperature with a magnetic moment corresponding to four unpaired electrons per chromium; however, as the temperature is lowered, magnetic susceptibility measurements show that **1** exhibits antiferromagnetic behavior with $J = -12.4 \text{ cm}^{-1}$ and $g = 1.99$. Chloride **1** can be converted to the mononuclear methyl complex $\text{CrMe}[\text{N}(\text{SiMe}_2\text{CH}_2\text{PPh}_2)_2]$ by reaction with MeLi . Under a hydrogen atmosphere, the methyl complex is converted to the dinuclear hydride derivative $\{[(\text{Ph}_2\text{PCH}_2\text{SiMe}_2)_2\text{N}]\text{Cr}\}_2(\mu\text{-H})_2$, **3**. A variable temperature magnetic susceptibility study shows that this species is very strongly antiferromagnetically coupled with $J = -139 \text{ cm}^{-1}$ and $g = 1.98$. The magnetic coupling correlates with the Cr–Cr distances observed in the solid state for these complexes: for **1**, the Cr–Cr distance is 3.64 while for the hydride **3** a much shorter distance of 2.641 Å is found. Crystals of $\{[(\text{Ph}_2\text{PCH}_2\text{SiMe}_2)_2\text{N}]\text{Cr}\}_2(\mu\text{-Cl})_2$, **1**, are triclinic, $a = 11.508(2) \text{ Å}$, $b = 12.267(3) \text{ Å}$, $c = 13.096(2) \text{ Å}$, $\alpha = 90.80(2)^\circ$, $\beta = 112.91(1)^\circ$, $\gamma = 109.52(2)^\circ$, $Z = 1$, and space group $P\bar{1}$; those of $\{[(\text{Ph}_2\text{PCH}_2\text{SiMe}_2)_2\text{N}]\text{Cr}\}_2(\mu\text{-H})_2$, **3**, are monoclinic, $a = 11.776(1) \text{ Å}$, $b = 19.061(2) \text{ Å}$, $c = 13.990(2) \text{ Å}$, $\beta = 103.153(10)^\circ$, $Z = 2$, and space group $P2_1/n$. The structures were solved by direct (chloride) and Patterson (hydride) methods and were refined by full-matrix least-squares procedures to $R = 0.064$ and 0.038 ($R_w = 0.037$ and 0.039) for 1832 and 3617 reflections with $I \geq 3\sigma(I)$, respectively.

Introduction

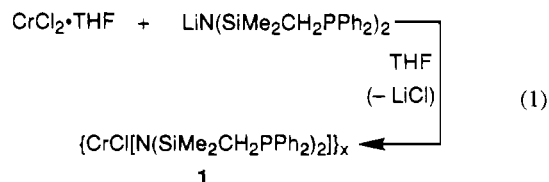
Communication between metal centers as manifested by magnetic interactions continues to be an area of intense current interest.¹ For example, the search for molecular ferromagnets² and investigations on the nature of metal ion sites in proteins³ rely on an understanding of how electron spin information is transmitted between metal centers either through ligands or through direct metal–metal bonds. A simple approach to study the phenomenon of magnetic exchange is to examine dinuclear metal complexes connected by different types of bridging ligands.^{4–6} While a number of studies have addressed this approach, noticeably absent are studies that include hydrides as bridging ligands.

Recently, we have initiated a study of paramagnetic organometallic complexes of Cr(II) and Cr(III) stabilized by the tridentate, anionic, mixed-donor ligand $\text{N}(\text{SiMe}_2\text{CH}_2\text{PPh}_2)_2$.⁷ In the course of this work, we came across two paramagnetic dinuclear Cr(II)–Cr(II) species that have remarkably similar geometries but very different room temperature magnetic moments. In fact, there is ample precedent in the literature to

suggest that dinuclear Cr(II)–Cr(II) complexes should be diamagnetic with potentially multiple metal–metal bond character.^{8,9} In an effort to understand the behavior of our dinuclear complexes, we subjected these derivatives to variable temperature magnetic susceptibility studies and also determined their solid-state structures. In this paper we detail this investigation, the results of which show that the hydride ligand is remarkably efficient in mediating magnetic exchange.

Synthesis and Structure of $\{[(\text{Ph}_2\text{PCH}_2\text{SiMe}_2)_2\text{N}]\text{Cr}\}_2(\mu\text{-Cl})_2$

A convenient starting material for the synthesis of chromium(II) paramagnetic complexes is $\text{CrCl}_2\cdot\text{THF}$.¹⁰ Addition of 1 equiv of $\text{LiN}(\text{SiMe}_2\text{CH}_2\text{PPh}_2)_2$ ¹¹ to a THF suspension of $\text{CrCl}_2\cdot\text{THF}$ results in the rapid formation of a dark blue solution. Removal of the THF and recrystallization from toluene afforded light blue crystals of empirical formula $\text{CrCl}[\text{N}(\text{SiMe}_2\text{CH}_2\text{PPh}_2)_2]$ (**1**) in high yield (eq 1). The reaction also proceeds



when using an anhydrous CrCl_2 suspension in THF, but the

* Recipient of a NSERC 1967 Fellowship (1992–1996).

† Professional Officer: UBC Crystallographic Service.

‡ Abstract published in *Advance ACS Abstracts*, October 15, 1994.

- (1) Willett, R. D.; Gatteschi, D.; Kahn, O. *Magneto-Structural Correlations in Exchange Coupled Systems*; Reidel: Dordrecht, The Netherlands, 1985.
- (2) Miller, J. S.; Dougherty, D. A. *Mol. Cryst. Liq. Cryst.* **1989**, *176*, 1.
- (3) Solomon, E. I. In *Metal Clusters in Proteins*; J. L. Que, Ed.; American Chemical Society: Washington, DC, 1988.
- (4) Kahn, O. *Angew. Chem., Int. Ed. Engl.* **1985**, *24*, 834.
- (5) Kato, M.; Muto, Y. *Coord. Chem. Rev.* **1988**, *92*, 45.
- (6) Moron, M. C.; Palacio, F.; Pons, J.; Casabo, J.; Solans, X.; Merabet, K. E.; Huang, D.; Shi, X.; Teo, B. K.; Carlin, R. L. *Inorg. Chem.* **1994**, *33*, 746.
- (7) Fryzuk, M. D. *Can. J. Chem.* **1992**, *70*, 2839.

- (8) Cotton, F. A.; Wilkinson, G. *Advanced Inorganic Chemistry*, 5th ed.; John Wiley & Sons: New York, 1988; pp 679.
- (9) Cotton, F. A.; Chen, H.; Daniels, L. M.; Feng, X. *J. Am. Chem. Soc.* **1992**, *114*, 8980.
- (10) Kern, R. J. *J. Inorg. Nucl. Chem.* **1962**, *24*, 1105.
- (11) Fryzuk, M. D.; MacNeil, P. A.; Rettig, S. J.; Secco, A. S.; Trotter, J. *Organometallics* **1982**, *1*, 918.

Table 1. Crystallographic Data^a

compound	{(Ph ₂ PCH ₂ SiMe ₂) ₂ N}Cr ₂ (μ-Cl) ₂ , 1 ^b	{(Ph ₂ PCH ₂ SiMe ₂) ₂ N}Cr ₂ (μ-H) ₂ , 3 ^c
formula	C ₆₀ H ₇₂ Cl ₂ Cr ₂ N ₂ P ₄ Si ₄	C ₆₀ H ₇₄ Cr ₂ N ₂ P ₄ Si ₄
fw	1232.38	1163.49
space group	P $\bar{1}$	P2 ₁ /n
a, Å	11.508(2)	11.776(1)
b, Å	12.267(4)	19.061(2)
c, Å	13.096(4)	13.990(2)
α, deg	90.80(2)	90
β, deg	112.91(1)	103.153(10)
γ, deg	109.52(2)	90
V, Å ³	1582.8(7)	3057.6(6)
Z	1	2
T, °C	22	21
ρ _c , g/cm ³	1.293	1.264
μ(MoKα), cm ⁻¹	6.42	5.77
final R	0.064	0.038
final R _w	0.037	0.039

^a $R = \sum ||F_o| - |F_c|| / \sum |F_o|$ and $R_w = (\sum w(|F_o| - |F_c|)^2 / \sum w|F_o|)^{1/2}$. ^b Siemens P3 diffractometer, takeoff angle 2.8°, aperture 2.0–2.5 × 2.0 mm at a distance of 210 mm from the crystal. ^c Rigaku AFC6S diffractometer, takeoff angle 6.0°, aperture 6.0 × 6.0 mm at a distance 285 mm from the crystal, stationary background counts at each end of the scan (scan/background time ratio 2:1).

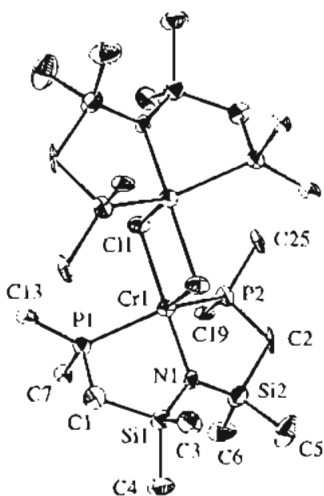


Figure 1. Molecular structure and numbering scheme for $\{[(Ph_2PCH_2SiMe_2)_2N]Cr\}_2(\mu-Cl)_2$, 1. The phenyl groups attached to the phosphorus atoms have been removed for clarity.

yield is substantially lower; a very soluble green byproduct, likely $Cr[N(SiMe_2CH_2PPh_2)_2]_2$, contaminates this latter reaction and complicates workup.

The ¹H NMR spectrum of 1 shows only broadened resonances from which no structural information could be determined. In addition, all of the Cr(II) compounds reported here are ESR silent both in solution and in frozen glass. However, crystals of 1 were obtained by slow evaporation of a saturated toluene solution; the results of the solid-state structure determination by X-ray crystallography are shown in Figure 1.

Structural analysis shows that 1 is dinuclear in the solid state, with a five-coordinate slightly distorted trigonal bipyramidal geometry around each chromium center. Each trigonal bipyramid is defined by the amide nitrogen of the tridentate ligand and one of the bridging chloride ligands in the axial sites and the two phosphine donors and the remaining bridging chloride in the equatorial positions. There is little distortion along the axial dimension as is evident from the Cl(1)–Cr(1)–N(1) angle of 179.2(3)° (Table 3); however, in the equatorial plane the P(1)–Cr(1)–P(2), Cl(1)*–Cr(1)–P(1), and Cl(1)*–Cr(1)–P(2) angles of 136.8(1), 107.4(1), and 115.4(1)°, respectively, do show large distortion from the ideal trigonal planar structure probably due to the large PPh₂ donors keeping as far apart as possible. The Cr–Cr distance of 3.64 Å (Table 2) is essentially

Table 2. Selected Bond Lengths (Å) for the Complexes $\{[(Ph_2PCH_2SiMe_2)_2N]Cr\}_2(\mu-Cl)_2$ (1) and $\{[(Ph_2PCH_2SiMe_2)_2N]Cr\}_2(\mu-H)_2$ (3)

	1	3
Cr(1)–Cr(1)*	3.64	2.641(1)
Cr(1)–H(1)		1.78(3)
Cr(1)–H(1)*		1.76(3)
Cr(1)–Cl(1)	2.397(3)	
Cr(1)–Cl(1)*	2.546(3)	
Cr(1)–P(1)	2.529(4)	2.537(1)
Cr(1)–P(2)	2.514(5)	2.513(1)
Cr(1)–N(1)	2.078(8)	2.076(2)
P(1)–C(1)	1.82(1)	1.819(4)
P(1)–C(7)	1.84(1)	1.831(4)
P(1)–C(13)	1.76(1)	1.825(4)
P(2)–C(2)	1.83(1)	1.813(3)
P(2)–C(19)	1.82(1)	1.831(3)
P(2)–C(25)	1.86(1)	1.829(4)
Si(1)–N(1)	1.745(9)	1.694(3)
Si(1)–C(1)	1.88(1)	1.900(4)
Si(1)–C(3)	1.87(1)	1.881(4)
Si(1)–C(4)	1.89(1)	1.870(4)
Si(2)–N(1)	1.629(9)	1.692(3)
Si(2)–C(2)	1.92(1)	1.903(4)
Si(2)–C(5)	1.86(1)	1.876(4)
Si(2)–C(6)	1.90(1)	1.858(4)

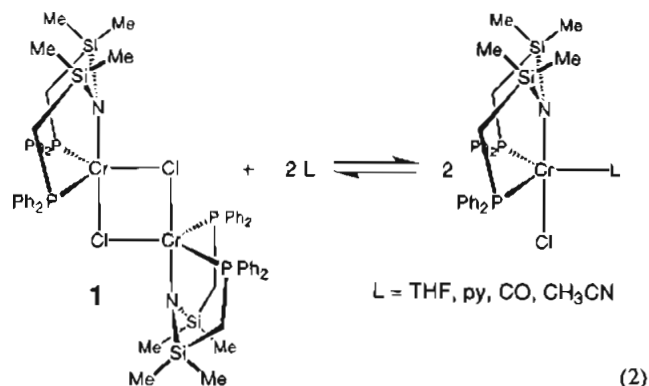
too long to invoke the existence of a metal–metal bond.¹²

The Cr–Cl distances of 2.396(4) and 2.556(4) Å indicate that the Cr₂(μ-Cl)₂ bridging core is highly unsymmetrical, similar to that found for [(dippe)CrCl]₂(μ-Cl)₂ (dippe = 1,2-bis-(diisopropylphosphino)ethane);¹³ the Cr–Cl–Cr angle is 94.6(1)°. Hence, the structure could be better described as two loosely associated monomers. As a result it is not surprising to note that in the mass spectrum of 1 only a monomer peak at *m/e* 615 is observed (as opposed to a dimer peak). Room temperature magnetic susceptibility measurements indicate a magnetic moment of 4.6 μ_B per chromium, consistent with an uncoupled high-spin d⁴ system (see variable temperature magnetic studies below). In addition, the bridge is easily cleaved by coordinating solvents or ligands. As a result, 1 is only slightly soluble in noncoordinating solvents such as benzene or toluene, but is extremely soluble in THF, acetonitrile, or pyridine. Addition of CO to a suspension of 1 in toluene results in the rapid solubilization of 1 as a yellow adduct. However, removal of THF, acetonitrile, or CO results in the recovery of blue, dimeric 1. In the case of pyridine, the resulting

(12) Vahrenkamp, H. *Angew. Chem., Int. Ed. Engl.* 1978, 17, 379.

(13) Hermes, A. R.; Girolami, G. S. *Inorg. Chem.* 1988, 27, 1775.

adduct is stable even with no excess pyridine present. Although suitable X-ray quality crystals could not be prepared, elemental analysis indicated that only one pyridine was bound, and therefore the formula $\text{CrCl}(\text{py})[\text{N}(\text{SiMe}_2\text{CH}_2\text{PPh}_2)_2]$ is suggested. The formation of five-coordinate, labile monomers is consistent with both the solid-state structural data and the vastly increased solubility in coordinating solvents such as THF (eq 2). This hypothesis is supported by the above-mentioned related



dimer $[(\text{dippe})\text{CrCl}]_2(\mu\text{-Cl})_2$ and the formation of the monomer $\text{Cr}(\text{NCCH}_3)\text{Cl}_2(\text{dippe})$ by reaction with acetonitrile.¹³

The Cr–P distances in **1** of 2.521(5) and 2.512(5) Å (Table 2) are longer than the Cr–P distances of 2.488(2) and 2.507(2) Å reported for $[(\text{dippe})\text{CrCl}]_2(\mu\text{-Cl})_2$.¹³ The Cr–N bond length of 2.08(1) Å is similar to that found in *trans*- $\text{Cr}[\text{N}(\text{SiMe}_2)_2]_2(\text{THF})_2$ (i.e., 2.089(12) Å).¹⁴ The N–Si bond lengths of 1.74(1) and 1.63(1) Å indicate firstly a degree of trigonal bipyramidal distortion and also a degree of $p\pi\text{-}d\pi$ interaction between the lone pair on the nitrogen amide and the silicon. The shorter of the two Si–N bond distances is the shortest reported, considerably shorter than in free disilazane (1.735 Å)¹⁵ but comparable to that found in *trans*- $\text{Cr}[\text{N}(\text{SiMe}_2)_2]_2(\text{THF})_2$ (1.674(17) Å).¹⁴

Synthesis and Structure of $\{[(\text{Ph}_2\text{PCH}_2\text{SiMe}_2)_2\text{N}]\text{Cr}\}_2(\mu\text{-H})_2$

The addition of MeLi to compound **1** affords the 12-electron mononuclear Cr(II) methyl derivative, $\text{CrCH}_3[\text{N}(\text{SiMe}_2\text{CH}_2\text{PPh}_2)_2]$ (**2**), in high yield. The structure and reactivity of this paramagnetic, square-planar complex is reported elsewhere.¹⁶ Reaction of the methyl derivative **2** with H₂ in toluene yields a color change from red to green with the formation of a dark olive-green precipitate having the empirical formula $\text{CrH}[\text{N}(\text{SiMe}_2\text{CH}_2\text{PPh}_2)_2]$ (**3**) (eq 3). The deuteride analogue of **3** was also prepared by reaction of **2** with D₂ and the IR spectrum clearly showed the Cr–H(D) stretching frequency shift from 1368 to 988 cm⁻¹. This value is clearly diagnostic of bridging hydrides. An oligonuclear structure was also indicated by the room temperature magnetic moment, which was determined to be 1.61 μ_B, evidently a coupled system (see variable temperature magnetic studies below). X-ray quality crystals of $\{[(\text{Ph}_2\text{PCH}_2\text{SiMe}_2)_2\text{N}]\text{Cr}\}_x(\mu\text{-H})_x$ were grown from a toluene solution of **2** to which was added 1 atm of H₂ and allowed to stand without stirring for 1 week. It is interesting to point out that other square planar Cr(II) alkyls of the formula $\text{CrR}_2(\text{dippe})$ are reported to

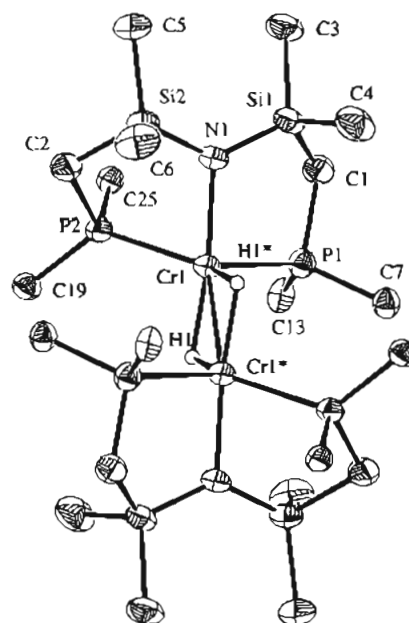
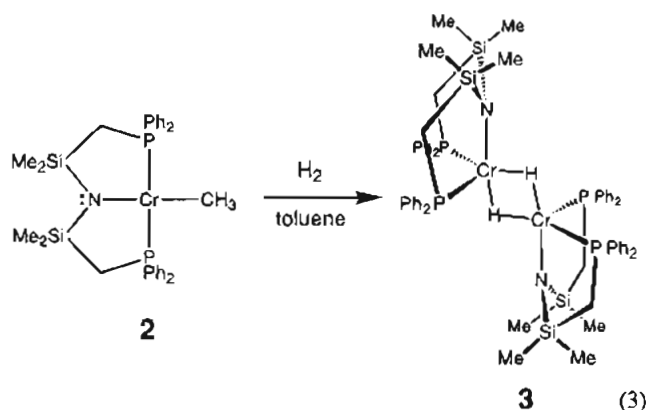


Figure 2. Molecular structure and numbering scheme for $\{[(\text{Ph}_2\text{PCH}_2\text{SiMe}_2)_2\text{N}]\text{Cr}\}_2(\mu\text{-H})_2$, **3**. The phenyl groups attached to the phosphorus atoms have been removed for clarity.

be unreactive to H₂.¹⁷ In fact, the only other example of a paramagnetic chromium(II) hydride is the $\text{Cp}^*_4\text{Cr}_4\text{H}_4$ cubane product recently communicated.¹⁸



Single-crystal X-ray structural analysis shows that **3** is dinuclear, with a distorted trigonal bipyramidal coordination around each of the Cr(II) centers (Figure 2). In comparison to the chloride-bridged dimer **1**, the presence of the smaller bridging hydrides in **3** results in larger distortions from pure trigonal bipyramidal geometry. For example, the axial amide nitrogen and hydride ligands are not quite linearly disposed as the N(1)–Cr(1)–H(1) angle is 173.2(8)° (Table 3). The equatorial ligands defined by the two phosphine donors and the other bridging hydride subtend the following angles: P(1)–Cr(1)–P(2), 106.09(4)°; P(1)–Cr(1)–H(1)*, 114.0(9)°; and P(2)–Cr(1)–H(1)*, 139.4(9)°. In contrast to the structure of **1** the $\text{Cr}_2(\mu\text{-H})_2$ bridging core is quite symmetrical; the Cr–H distances of 1.78(3) and 1.76(3) Å (Table 2) and the H(1)–Cr(1)–H(1)* angle of 83(1)° describe the bridge. The Cr–Cr distance of 2.641(1) Å in **3** is 1 Å shorter than in **1**, and hence the potential existence of a Cr–Cr bond cannot be ruled out. The Cr–P distances of 2.513(1) and 2.537(1) Å are comparable

(14) Bradley, D. C.; Hursthouse, M. B.; Newing, C. W.; Welch, A. J. *J. Chem. Soc., Chem. Commun.* **1972**, 567.

(15) Robiette, A. G.; Sheldrick, G. M.; Sheldrick, W. S.; Beagley, B.; Cruickshank, D. W. J.; Monaghan, J. J.; Aylett, B. J.; Ellis, I. A. *J. Chem. Soc., Chem. Commun.* **1968**, 909.

(16) Fryzuk, M. D.; Leznoff, D. B.; Rettig, S. J. Manuscript in preparation.

(17) Hermes, A. R.; Morris, R. J.; Girolami, G. S. *Organometallics* **1988**, *7*, 2372.

(18) Heintz, R. A.; Haggerty, B. S.; Wan, H.; Rheingold, A. L.; Theopold, K. H. *Angew. Chem., Int. Ed. Engl.* **1992**, *31*, 1077.

Table 3. Selected bond angles (deg) for the complexes

$\{[(\text{Ph}_2\text{PCH}_2\text{SiMe}_2)_2\text{N}]\text{Cr}\}_2(\mu\text{-Cl})_2$ (**1**) and
 $\{[(\text{Ph}_2\text{PCH}_2\text{SiMe}_2)_2\text{N}]\text{Cr}\}_2(\mu\text{-H})_2$ (**3**)

	1	3
Cr(1)–Cr(1)*–H(1)		41.6(8)
Cr(1)–Cr(1)*–H(1)*		41.9(9)
P(1)–Cr(1)–H(1)		97.6(8)
P(1)–Cr(1)–H(1)*		114.0(9)
P(2)–Cr(1)–H(1)		97.7(8)
P(2)–Cr(1)–H(1)*		139.4(9)
N(1)–Cr(1)–H(1)		173.2(8)
N(1)–Cr(1)–H(1)*		96.3(9)
H(1)–Cr(1)–H(1)*		83(1)
Cr(1)*–Cr(1)–P(1)		111.12(4)
Cr(1)*–Cr(1)–P(2)		126.65(4)
Cr(1)*–Cr(1)–N(1)		137.87(8)
Cl(1)–Cr(1)–Cl(1)*	85.4(1)	
Cl(1)–Cr(1)–P(1)	95.8(1)	
Cl(1)–Cr(1)–P(2)	93.3(1)	
Cl(1)–Cr(1)–N(1)	179.2(3)	
Cl(1)*–Cr(1)–P(1)	107.4(1)	
Cl(1)*–Cr(1)–P(2)	115.4(1)	
Cl(1)*–Cr(1)–N(1)	94.8(2)	
Cr(1)–Cl(1)–Cr(1)*	94.6(1)	
P(1)–Cr(1)–P(2)	136.8(1)	106.09(4)
P(1)–Cr(1)–N(1)	84.9(3)	88.75(8)
P(2)–Cr(1)–N(1)	85.9(3)	77.95(8)
Cr(1)–P(1)–C(1)	100.2(4)	101.9(1)
Cr(1)–P(1)–C(7)	113.3(4)	121.9(1)
Cr(1)–P(1)–C(13)	127.6(4)	117.6(1)
C(1)–P(1)–C(7)	104.7(5)	105.8(2)
C(1)–P(1)–C(13)	107.7(6)	107.2(2)
C(7)–P(1)–C(13)	101.4(6)	101.4(2)
Cr(1)–P(2)–C(2)	101.9(4)	99.9(1)
Cr(1)–P(2)–C(19)	115.6(5)	125.8(1)
Cr(1)–P(2)–C(25)	126.3(4)	116.4(1)
C(2)–P(2)–C(19)	103.6(6)	106.6(2)
C(2)–P(2)–C(25)	105.7(7)	105.5(2)
C(19)–P(2)–C(25)	101.3(5)	100.9(2)
N(1)–Si(1)–C(1)	109.2(5)	106.5(1)
N(1)–Si(1)–C(3)	113.5(5)	116.3(2)
N(1)–Si(1)–C(4)	113.2(5)	111.7(2)
C(1)–Si(1)–C(3)	106.7(6)	104.6(2)
C(1)–Si(1)–C(4)	108.9(6)	111.4(2)
C(3)–Si(1)–C(4)	105.0(5)	106.2(2)
N(1)–Si(2)–C(2)	109.6(5)	105.2(1)
N(1)–Si(2)–C(5)	115.5(6)	116.8(2)
N(1)–Si(2)–C(6)	113.9(6)	113.2(2)
C(2)–Si(2)–C(5)	103.3(7)	108.3(2)
C(2)–Si(2)–C(6)	106.3(5)	106.9(2)
C(5)–Si(2)–C(6)	107.4(7)	105.5(2)
Cr(1)–N(1)–Si(1)	114.6(5)	116.7(1)
Cr(1)–N(1)–Si(2)	122.2(5)	112.1(1)
Si(1)–N(1)–Si(2)	123.0(5)	130.8(1)
P(1)–C(1)–Si(1)	111.7(6)	111.3(2)
P(2)–C(2)–Si(2)	106.4(6)	107.4(2)

to those found in **1** and in other known high-spin Cr(II) phosphines^{13,17} and considerably longer than that found in low-spin Cr(II) systems.¹⁹ The Cr–N bond length of 2.076(2) Å is similar to that found in $\text{Cr}[\text{N}(\text{SiMe}_3)_2]_2(\text{THF})_2$ and this information, coupled with the comparatively short N–Si bonds of 1.694(3) and 1.692(3) Å again indicates that the lone pair on the amide is not participating in the Cr–N bond, but is delocalized by the adjacent silicons.

Magnetic Susceptibility Studies

The magnetic susceptibility (per mole of dimer), χ_m , versus temperature plot for **1** reveals a broad maximum in susceptibility around 66 K consistent with the presence of significant antiferromagnetic coupling in the compound (Figure 3). The

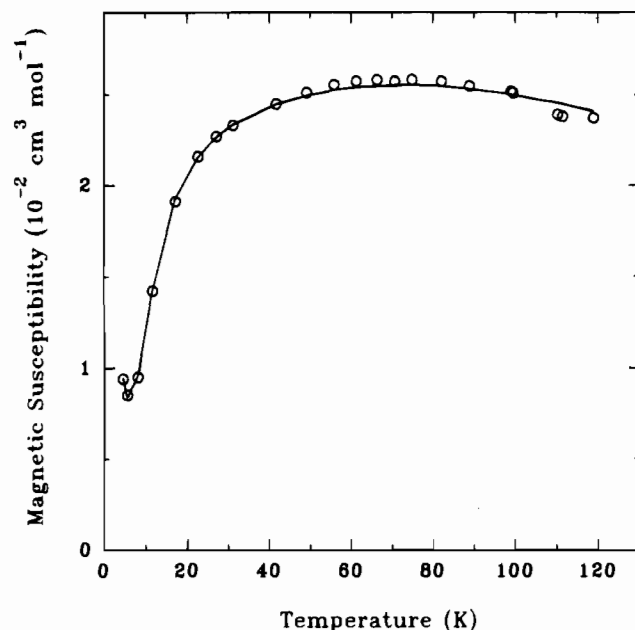


Figure 3. Magnetic susceptibility (per mole of dimer) versus temperature plot for **1**. The line was generated using the Heisenberg dimer model with $J = -12.4 \text{ cm}^{-1}$, $g = 1.99$, and $P = 0.007$.

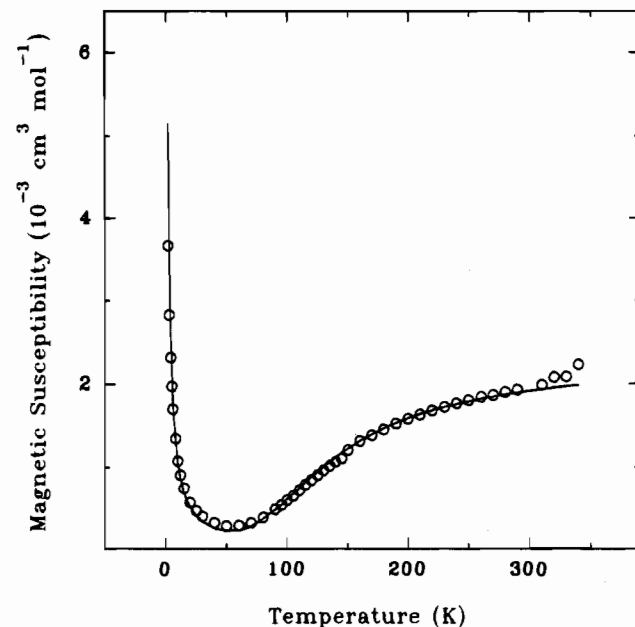


Figure 4. Magnetic susceptibility (per mole of dimer) versus temperature plot for **3**. The line was generated using the Heisenberg dimer model with $J = -139 \text{ cm}^{-1}$, $g = 1.98$, and $P = 0.0017$. Experimental data were corrected for $\text{TIP} = 300 \times 10^{-6} \text{ cm}^3 \text{ mol}^{-1}$.

corresponding plot for **3** (Figure 4) indicates the approach to a maximum at temperatures above 300 K. Unfortunately this compound is not sufficiently thermally stable above this temperature to permit meaningful susceptibility measurements in this region. Nonetheless, the general features of the χ_m vs T plot at temperatures below 300 K as well as the observation that the χ_m values for **3** are an order of magnitude smaller than those for **1** suggest even stronger antiferromagnetic exchange coupling in **3**. The increase in susceptibility with decreasing temperature at the lowest temperatures studied as observed for both **1** and **3** likely arises from the presence of paramagnetic impurity. This is commonly seen in studies of antiferromagnetically coupled systems.²⁰ Although the paramagnetic tail seen in the plot for **3** (Figure 4) gives the appearance of

(19) Girolami, G. S.; Salt, J. E.; Wilkinson, G. *J. Am. Chem. Soc.* **1983**, *105*, 5954.

indicating a large amount of impurity, this is not the case. The antiferromagnetic coupling in this compound is so strong that, at the lowest temperatures studied, the bulk of the sample is effectively diamagnetic, making paramagnetic contributions from even traces of impurities observable. In fact, the data for this compound (as described below) show that the impurity level is less than 0.2% of the chromium present.

The magnetic susceptibility data for **1** and **3** were analyzed employing the dimeric Heisenberg model for $S = 2$

$$\chi_{\text{dimer}} = \left(\frac{Ng^2\mu_B^2}{kT} \right) \left(\frac{2e^{2x} + 10e^{6x} + 28e^{12x} + 60e^{20x}}{1 + 3e^{2x} + 5e^{6x} + 7e^{12x} + 9e^{20x}} \right)$$

where $x = J/kT$.²¹ To account for the presence of paramagnetic impurity the expression was combined with the Curie law term

$$\chi_{\text{para}} = \frac{Ng^2\mu_B^2 S(S+1)}{3kT}$$

according to

$$\chi_m = [1 - P]\chi_{\text{dimer}} + P\chi_{\text{para}}$$

where P represents the fraction of paramagnetic impurity. Fits of the experimental data to the model were achieved using a nonlinear least-squares procedure with the following as the function minimized:

$$F = \left[\frac{1}{n} \sum_{i=1}^n \frac{(\chi_i^{\text{obs}} - \chi_i^{\text{calc}})^2}{(\chi_i^{\text{obs}})^2} \right]^{1/2}$$

The F value provides a measure of the goodness of fit between experiment and theory.

Experimental susceptibility versus temperature data for **1** are compared with the best fit results from theory (Figure 3) with $J = -12.4 \text{ cm}^{-1}$, $g = 1.99$, and $P = 0.007$ ($F = 0.0144$). A g value slightly less than the free spin value is not unexpected for a d^4 system.²² The Cr–Cr separation of 3.64 Å would preclude direct metal orbital overlap as the mechanism for exchange in this compound requiring, therefore, a superexchange mechanism via the bridging chloro-ligands. The exchange coupling constant, J , is comparable in magnitude to values reported some years ago for some extended chain and sheet chloro-bridged Cr(II) systems.^{23,24} The compounds Cs[CrCl₃], [(CH₃)₄N][CrCl₃], and [C₅H₅NH]₂[CrCl₄] are reported to be antiferromagnetic with J values of approximately -25 , -12.5 , and -6.5 cm^{-1} , respectively. The complex Cs[CrCl₃(OH₂)₂], which is thought to have a dimeric, double chloro-bridged structure similar to that of **1**, is antiferromagnetic with $J = -3 \text{ cm}^{-1}$.²³ It is somewhat surprising that the magnitude of J is so large for **1** considering the unsymmetrical nature of the chloro bridges. Unfortunately we know of no other report on a chloro-bridged dimeric Cr(II) system where both detailed magnetic and single-crystal X-ray diffraction studies have been reported. A single-crystal X-ray diffraction study of [CrCl₂(dippe)]₂ (dippe = 1,2-bis(diisopropylphosphino)ethane) revealed a dimeric

structure with unsymmetrical bridging chloro ligands (Cr–Cl distances of 2.380 and 2.606 Å), much like the situation in **1**.¹³ Unfortunately, the only magnetic study reported on this compound is a room temperature measurement on a solution in acetonitrile. Under these conditions a mononuclear acetonitrile adduct is formed and the magnetic study merely confirms the presence of a high-spin d^4 metal center. Finally we note that chloro-bridged Cr(II) systems also provide examples of ferromagnetism, a relatively rare phenomenon in metal complex chemistry. The compounds M₂[CrCl₄] ($M = \text{K, Rb, Cs}$) have structures involving two-dimensional networks of Cr and Cl atoms, each Cr being surrounded by four others, with 180° Cr–Cl–Cr bonds. Magnetic studies on these systems have revealed ferromagnetic exchange with J values estimated to lie in the range 6.5–8.5 cm^{-1} .²⁵

The structure of **3** reveals a bimetallic system with the metals separated by a symmetrical double hydride bridge and a Cr–Cr separation of only 2.641(1) Å. It is not surprising therefore that the metals are more strongly coupled antiferromagnetically than in **1**. The magnetic susceptibilities were analyzed as for **1** with the exception that the experimental data were first corrected for temperature independent paramagnetism (TIP).²² The best fit between experiment and theory, employing a TIP correction of $300 \times 10^{-6} \text{ cm}^3 \text{ mol}^{-1}$ (per dimer unit), shown in Figure 4, yielded $J = -139 \text{ cm}^{-1}$, $g = 1.98$, and $P = 0.0017$ with $F = 0.0989$. Employing a larger TIP correction of $400 \times 10^{-6} \text{ cm}^3 \text{ mol}^{-1}$ yields a better fit ($F = 0.0521$) with $J = -150 \text{ cm}^{-1}$, $g = 2.069$, and $P = 0.0014$. However, we favor the former fit in the light of the more realistic g value it generates. In either case it is clear that the absolute value of the exchange integral, $|J|$, is at least of the order of 140 cm^{-1} and is considerably greater than that observed for **1**.

The magnetic analysis given above does not permit us to distinguish between direct metal orbital overlap and ligand mediated superexchange as potential mechanisms for the interaction. Comparisons with related systems could prove useful in this regard; however, the paucity of relevant structural and magnetic studies, particularly on hydride-bridged complexes, limits this possibility. Of some relevance is the recent characterization of a paramagnetic hydride-bridged chromium(II) complex with a cubane structure.¹⁸ The magnetic properties are reported to be almost ideal Curie-type paramagnetism, suggesting no significant antiferromagnetic exchange between metal centers. In this case the metals are linked by single triply-bridging hydrides and the average Cr–Cr distance is 2.715 Å, significantly longer than observed in **3**. Magnetic studies on bimetallic Cr(II) species involving Cr₂(μ -OR)₂ cores (where OR is aryloxy or alkoxide) have been analyzed qualitatively and the results reveal dependence of the strength of antiferromagnetic coupling on the Cr–Cr distance and the nature of the bridging group; however no definite magnetostructural correlations have been revealed in this work.^{26,27} An amide bridged dimer containing a Cr₂(μ -NR₂)₂ core has also been studied magnetically but only at high temperatures.²⁸ The compound exhibits Curie–Weiss behavior indicative of antiferromagnetic exchange between metal centers.

(20) Otiemo, T.; Rettig, S. J.; Thompson, R. C.; Trotter, J. *Inorg. Chem.* **1993**, *32*, 4384.

(21) O'Connor, C. J. *Prog. Inorg. Chem.* **1982**, *29*, 203.

(22) Mabbs, F. E.; Machin, D. J. *Magnetism and Transition Metal Complexes*; Chapman and Hall: London, 1973.

(23) Larkworthy, L. F.; Trigg, J. K.; Yavari, A. J. *Chem. Soc., Dalton Trans.* **1975**, 1879.

(24) Leed, D. H.; Machin, D. J. *J. Chem. Soc., Chem. Commun.* **1974**, 866.

(25) Gregson, A. K.; Day, P.; Leech, D. H.; Fair, M. J.; Gardner, W. E. *J. Chem. Soc., Dalton Trans.* **1975**, 1306.

(26) Edema, J. J. H.; Gambarotta, S. *Comments Inorg. Chem.* **1991**, *11*, 195.

(27) Edema, J. J. H.; Gambarotta, S.; Smeets, W. J. J.; Spek, A. L. *Inorg. Chem.* **1991**, *30*, 1380.

(28) Edema, J. J. H.; Gambarotta, S.; Spek, A. L. *Inorg. Chem.* **1989**, *28*, 812.

Table 4. Final Atomic Coordinates and B_{eq} (\AA^2) for $\{[(\text{Ph}_2\text{PCH}_2\text{SiMe}_2)_2\text{N}]\text{Cr}\}_2(\mu\text{-Cl})_2$, **1**

atom	x	y	z	B_{eq}^a
Cr(1)	0.3926(2)	0.3623(2)	0.4039(2)	3.01(6)
Cl(1)	0.6125(3)	0.4356(3)	0.5583(2)	3.77(9)
P(1)	0.4779(3)	0.3653(3)	0.2523(3)	2.92(9)
P(2)	0.2932(4)	0.2111(3)	0.5048(3)	3.60(10)
Si(1)	0.1881(4)	0.3623(3)	0.1519(3)	3.5(1)
Si(2)	0.0702(4)	0.2032(3)	0.2840(3)	4.2(1)
N(1)	0.2008(9)	0.2973(7)	0.2715(7)	2.7(2)
C(1)	0.356(1)	0.4101(9)	0.1424(9)	3.6(3)
C(2)	0.114(1)	0.193(1)	0.440(1)	4.3(4)
C(3)	0.144(1)	0.496(1)	0.1528(10)	5.0(4)
C(4)	0.053(1)	0.262(1)	0.018(1)	5.6(4)
C(5)	-0.082(1)	0.243(1)	0.239(1)	7.6(5)
C(6)	0.015(1)	0.049(1)	0.210(1)	6.2(4)
C(7)	0.452(1)	0.2182(9)	0.1914(9)	2.8(3)
C(8)	0.322(1)	0.140(1)	0.129(1)	4.5(4)
C(9)	0.305(1)	0.031(1)	0.085(1)	5.3(4)
C(10)	0.403(2)	-0.004(1)	0.096(1)	5.5(5)
C(11)	0.527(2)	0.069(1)	0.160(2)	8.7(6)
C(12)	0.557(1)	0.184(1)	0.211(1)	6.4(5)
C(13)	0.640(1)	0.448(1)	0.261(1)	3.7(4)
C(14)	0.761(1)	0.492(1)	0.361(1)	4.7(4)
C(15)	0.883(1)	0.548(1)	0.367(1)	5.3(4)
C(16)	0.905(2)	0.570(1)	0.272(2)	5.9(5)
C(17)	0.790(2)	0.530(1)	0.170(1)	5.7(5)
C(18)	0.663(1)	0.471(1)	0.166(1)	5.0(4)
C(19)	0.290(1)	0.0649(10)	0.4738(10)	3.2(3)
C(20)	0.347(2)	0.045(1)	0.401(1)	6.0(5)
C(21)	0.342(2)	-0.065(2)	0.375(1)	7.3(6)
C(22)	0.278(2)	-0.157(1)	0.419(1)	6.3(5)
C(23)	0.221(2)	-0.139(1)	0.488(1)	6.8(6)
C(24)	0.231(2)	-0.027(1)	0.516(1)	5.4(5)
C(25)	0.341(2)	0.2260(10)	0.659(1)	3.4(4)
C(26)	0.483(2)	0.253(1)	0.724(1)	4.9(4)
C(27)	0.525(2)	0.261(1)	0.847(1)	6.1(5)
C(28)	0.429(2)	0.243(1)	0.888(2)	7.7(7)
C(29)	0.296(2)	0.216(1)	0.820(2)	6.2(5)
C(30)	0.254(2)	0.210(1)	0.706(1)	5.7(5)

^a $B_{eq} = \frac{8}{3} \pi^2 (U_{11}(aa^*)^2 + U_{22}(bb^*)^2 + U_{33}(cc^*)^2 + 2U_{12}aa^*bb^* \cos \gamma + 2U_{13}aa^*cc^* \cos \beta + 2U_{23}bb^*cc^* \cos \alpha)$.

Conclusions

The results of this study show that dinuclear chromium(II) complexes containing two single atom bridges can participate in magnetic exchange; however, the extent of the magnetic coupling is highly dependent on the nature of the bridge. For complex **1** having chloride bridges, the coupling is rather small and comparable to other halide-bridged complexes of Cr(II). However, the magnetic exchange coupling for the dinuclear hydride complex **3** is an order of magnitude larger than that of **1** and suggests the possibility that hydride ligands can be extremely efficient mediators of magnetic information. More importantly, to our knowledge, this is the first detailed magnetic study of a dinuclear paramagnetic metal hydride.

Experimental Section

General Procedures. The preparation of the lithium salt $\text{LiN}(\text{SiMe}_2\text{CH}_2\text{PPh}_2)_2$ has been previously described.¹¹ All other reagents were obtained from commercial sources and used as received. $\text{CrCl}_2 \cdot \text{THF}$ was prepared by Soxhlet extraction of commercial CrCl_2 (Strem) with THF.¹⁰ Unless otherwise stated all manipulations were performed under an atmosphere of dry, oxygen-free dinitrogen by means of standard Schlenk or glovebox techniques. The glovebox used was a Vacuum Atmospheres HE-553-2 device equipped with a MO-40-2H purification system and a -40 °C freezer. Microanalyses (C, H, and N) were performed by Mr. P. Borda of this department. Hexanes, toluene, pentane, Et_2O , and THF were heated to reflux over CaH_2 prior to a final distillation from either sodium metal or sodium benzophenone ketyl under an Ar atmosphere. Deuterated solvents were dried by

Table 5. Final Atomic Coordinates and B_{eq} (\AA^2) for $\{[(\text{Ph}_2\text{PCH}_2\text{SiMe}_2)_2\text{N}]\text{Cr}\}_2(\mu\text{-H})_2$, **3**

atom	x	y	z	B_{eq}^a
Cr(1)	0.08001(4)	0.00321(3)	0.08307(4)	3.16(1)
P(1)	0.09143(8)	0.12541(5)	0.15648(7)	3.64(2)
P(2)	0.10459(7)	-0.08053(5)	0.22508(7)	3.49(2)
Si(1)	0.33474(8)	0.07295(6)	0.14575(8)	4.11(2)
Si(2)	0.30781(8)	-0.08755(6)	0.12969(8)	4.06(2)
N(1)	0.2601(2)	-0.0037(1)	0.1285(2)	3.52(6)
C(1)	0.2472(3)	0.1350(2)	0.2073(3)	4.55(9)
C(2)	0.2100(3)	-0.1406(2)	0.1938(3)	4.67(10)
C(3)	0.4833(3)	0.0701(2)	0.2311(3)	5.9(1)
C(4)	0.3564(4)	0.1099(2)	0.0273(3)	6.7(1)
C(5)	0.4634(3)	-0.1042(2)	0.1939(3)	5.8(1)
C(6)	0.2912(4)	-0.1254(2)	0.0049(3)	6.6(1)
C(7)	0.0474(3)	0.2033(2)	0.0805(2)	3.85(9)
C(8)	0.0916(5)	0.2162(3)	0.0008(3)	8.3(2)
C(9)	0.0568(6)	0.2730(3)	-0.0602(4)	9.2(2)
C(10)	-0.0249(5)	0.3170(3)	-0.0421(4)	7.3(1)
C(11)	-0.0714(5)	0.3046(3)	0.0326(4)	9.5(2)
C(12)	-0.0350(4)	0.2486(3)	0.0959(4)	7.9(2)
C(13)	0.0181(3)	0.1404(2)	0.2564(3)	4.28(10)
C(14)	0.0636(4)	0.1820(2)	0.3364(3)	6.2(1)
C(15)	0.0046(6)	0.1921(3)	0.4096(4)	8.7(2)
C(16)	-0.1012(6)	0.1609(3)	0.4024(4)	8.8(2)
C(17)	-0.1500(4)	0.1201(3)	0.3242(4)	6.9(1)
C(18)	-0.0887(4)	0.1093(2)	0.2504(3)	5.1(1)
C(19)	-0.0105(3)	-0.1346(2)	0.2558(2)	3.74(9)
C(20)	-0.1240(3)	-0.1151(2)	0.2237(3)	5.4(1)
C(21)	-0.2129(3)	-0.1560(3)	0.2447(4)	6.9(1)
C(22)	-0.1872(4)	-0.2160(3)	0.2969(3)	6.4(1)
C(23)	-0.0742(4)	-0.2361(2)	0.3307(3)	6.0(1)
C(24)	0.0140(3)	-0.1957(2)	0.3109(3)	5.0(1)
C(25)	0.1739(3)	-0.0453(2)	0.3458(2)	3.76(8)
C(26)	0.2890(4)	-0.0540(3)	0.3895(3)	7.7(1)
C(27)	0.3365(4)	-0.0243(4)	0.4809(4)	9.4(2)
C(28)	0.2719(5)	0.0143(3)	0.5282(3)	7.2(1)
C(29)	0.1579(5)	0.0241(2)	0.4867(3)	6.7(1)
C(30)	0.1085(3)	-0.0064(2)	0.3956(3)	5.6(1)
H(1)	-0.074(2)	-0.002(1)	0.044(2)	3.6(6)

^a $B_{eq} = \frac{8}{3} \pi^2 (U_{11}(aa^*)^2 + U_{22}(bb^*)^2 + U_{33}(cc^*)^2 + 2U_{12}aa^*bb^* \cos \gamma + 2U_{13}aa^*cc^* \cos \beta + 2U_{23}bb^*cc^* \cos \alpha)$.

activated 3 Å molecular sieves; oxygen was removed by trap to trap distillation and three freeze-pump-thaw cycles. All magnetic moments reported in the experimental section were determined from Gouy measurements performed on a Johnson Matthey MSB-1 apparatus at room temperature. Variable temperature magnetic susceptibility studies were performed as detailed below.

$\{[(\text{Ph}_2\text{PCH}_2\text{SiMe}_2)_2\text{N}]\text{Cr}\}_2(\mu\text{-Cl})_2$. To a stirred suspension of $\text{CrCl}_2 \cdot \text{THF}$ (2.55 g, 0.0111 mol) in 30 mL of THF was added dropwise a 20 mL THF solution of $\text{LiN}(\text{SiMe}_2\text{CH}_2\text{PPh}_2)_2$ (5.44 g, 0.0101 mol) over 5 min, at room temperature. The relatively insoluble light blue $\text{CrCl}_2 \cdot \text{THF}$ rapidly dissolves to generate the dark blue to indigo initial product $\text{Cr}(\text{THF})\text{Cl}[\text{N}(\text{SiMe}_2\text{CH}_2\text{PPh}_2)_2]$. After 10 min, the THF was removed in vacuo to yield a light blue-green solid, which after filtration through Celite, was recrystallized from minimum toluene/THF (95:5). Yield: 5.5 g of turquoise prisms (88%). ^1H NMR (C_7D_8): Too insoluble. $^{31}\text{P}\{^1\text{H}\}$ NMR (THF, ppm): -22.1 (100 Hz line width). MS: m/e 615 (M^+). UV-vis (toluene): 284 nm ($\epsilon = 3260$), 342 (shoulder, $\epsilon = 450$), 522 ($\epsilon = 140$), 688 ($\epsilon = 160$). Anal. Calcd for $\text{C}_{30}\text{H}_{36}\text{ClCrN}_2\text{P}_2\text{Si}_2$: C, 58.48; H, 5.89; N, 2.27. Found: C, 58.64; H, 5.81; N, 2.34. $\mu = 4.6 \mu_B$.

$\text{Cr}(\text{py})\text{Cl}[\text{N}(\text{SiMe}_2\text{CH}_2\text{PPh}_2)_2]$. To a stirred light blue suspension of $\{[(\text{Ph}_2\text{PCH}_2\text{SiMe}_2)_2\text{N}]\text{Cr}\}_2(\mu\text{-Cl})_2$ (150 mg, 0.244 mmol) in toluene was added pyridine (0.3 mL, 3.71 mmol) to yield a dark green solution. Removal of the solvent in vacuo yielded a green oil. Addition of hexanes and filtration through Celite yielded a green solution, which upon cooling formed purple crystals after 2 days. Yield: 140 mg (83%). Anal. Calcd for $\text{C}_{35}\text{H}_{41}\text{ClCrN}_2\text{P}_2\text{Si}_2$: C, 60.46; H, 5.94; N, 4.03. Found: C, 60.19; H, 5.89; N, 3.90.

$\text{CrCH}_3[\text{N}(\text{SiMe}_2\text{CH}_2\text{PPh}_2)_2]$. To a stirred solution of $\{[(\text{Ph}_2\text{PCH}_2\text{SiMe}_2)_2\text{N}]\text{Cr}\}_2(\mu\text{-Cl})_2$ (1.4 g, 2.28 mmol) in 20 mL of THF was added dropwise MeLi (8.2 mL, 0.28 M in ether, 2.30 mmol) at -78 °C. The

dark blue-indigo solution quickly turned dark brown. The reaction was allowed to warm to room temperature and then the THF was removed in vacuo over 1 h to yield a brown tar. Extraction with hexanes and filtering through Celite yielded brown parallelogram prisms after 5 min., which were washed with cold hexanes. Yield: 1.36 g (90%). MS: *m/e* 580 ($M^+ - H$). Anal. Calcd for $C_{31}H_{39}CrNP_2Si_2$: C, 62.50; H, 6.60; N, 2.35. Found: C, 62.44; H, 6.62; N, 2.47. $\mu = 4.7 \mu_B$.

$\{[(Ph_2PCH_2SiMe_2)_2N]Cr\}_2(\mu-H)_2$. A solution of $CrCH_3[N(SiMe_2CH_2PPh_2)_2]$ (0.33 g, 0.569 mmol) in toluene (30 mL) was placed in a thick-walled bomb and placed under 4 atm of H_2 (or D_2). The brown-red solution turned olive green over 1 h and a precipitate began to form. After 12 h, the H_2 was removed and the green-black precipitate was collected on a fine frit and washed with cold THF. Yield: 0.25 g (78%). IR: 1368 (ν_{C-H}), (988, ν_{C-D}). MS: *m/e* 580 ($M^+ - H$). Anal. Calcd for $C_{30}H_{37}CrNP_2Si_2$: C, 61.94; H, 6.41; N, 2.41. Found: C, 62.09; H, 6.42; N, 2.54. $\mu = 1.6 \mu_B$.

In order to obtain crystals suitable for X-ray diffraction, 75 mg of $CrCH_3[N(SiMe_2CH_2PPh_2)_2]$ was dissolved in 10 mL of toluene in a large (125 mL) Erlenmeyer flask equipped with a needle valve adapter and was carefully placed under 1 atm of H_2 and left for 4 days. Large cubic X-ray quality crystals slowly deposited and were submitted for structural analysis.

Variable Temperature Magnetic Susceptibility Studies. Magnetic susceptibility measurements on a powdered sample of **1** were made at an applied field of 9225 Oe over the temperature range 4.6–119 K using a PAR Model 155 vibrating-sample magnetometer as previously described.²⁹ For **3**, magnetic susceptibilities on a powdered sample over the range 2–340 K and at a field of 10 000 Oe were measured using a Quantum Design (MPMS) SQUID magnetometer. The sample holder, made from PVC, was specially designed to possess a constant cross-sectional area. Magnetic susceptibilities were corrected for sample holder background signal and for the diamagnetism of all atoms. The rather low values of susceptibility measured for **3** required that a correction be made for temperature independent paramagnetism in this case (see Discussion).

X-ray Crystallographic Analyses of $\{[(Ph_2PCH_2SiMe_2)_2N]Cr\}_2(\mu-Cl)_2$, **1, and $\{[(Ph_2PCH_2SiMe_2)_2N]Cr\}_2(\mu-H)_2$, **3**.** Crystallographic data appear in Table 1. The final unit cell parameters were obtained by least-squares on the setting angles for 25 reflections with $2\theta = 18-$

25 and 30.0–39.4°, respectively, for **1** and **3**. The intensities of three standard reflections, measured every 200 reflections throughout the data collections, remained constant for **1** and decayed uniformly by 1.7% for **3**. The data were processed,³⁰ corrected for Lorentz and polarization effects, decay (for **3**), and absorption (empirical: DIFABS³¹ for **1**; based on azimuthal scans for three reflections for **3**).

The chloride structure was solved by direct methods and the hydride structure by conventional heavy atom methods. In both structures the binuclear complexes have exact inversion symmetry. The non-hydrogen atoms of both structures were refined with anisotropic thermal parameters. The metal hydride atom of **3** was refined with an isotropic thermal parameter. All other hydrogen atoms were fixed in idealized positions (staggered methyl groups, $C-H = 0.99 \text{ \AA}$, $B_H = 1.2B_{\text{bonded atom}}$). A correction for secondary extinction was applied for **3**, the final value of the extinction coefficient being $4.4(26) \times 10^{-8}$. Selected bond lengths and bond angles appear in Tables 2 and 3, respectively; Tables 4 and 5 list the final atomic coordinates. Neutral atom scattering factors and anomalous dispersion corrections for all atoms were taken from ref 32. Complete bond lengths and angles, hydrogen atom parameters, anisotropic thermal parameters, torsion angles, intermolecular contacts, and least-squares planes are included as supplementary material.

Acknowledgment. Financial support was provided by NSERC of Canada in the form of Research grants (to M.D.F. and R.C.T.) and a 1967 Science and Engineering Scholarship (to D.B.L.). We also acknowledge the assistance of Drs. Stephen Geib and Charles Campana at the second ACA Summer Course for Crystallography.

Supplementary Material Available: Complete tables of crystallographic data, bond lengths and bond angles, hydrogen atom parameters, anisotropic thermal parameters, torsion angles, intermolecular contacts, and least-squares planes and full diagrams with phenyl groups included (37 pages). Ordering information is given on any current masthead page.

(30) *teXsan: Crystal Structure Analysis Package*; Molecular Structure Corporation: The Woodlands, TX, 1985 & 1992.

(31) Walker, N.; Stuart, L. *Acta Crystallogr.* **1983**, A39, 158.

(32) *International Tables for Crystallography*; Kluwer Academic Publishers: Boston, MA, 1992; Vol. C, pp 200–206 and 219–222.

(29) Haynes, J. S.; Oliver, K. W.; Rettig, S. J.; Thompson, R. C.; Trotter, J. *Can. J. Chem.* **1984**, 62, 891.